Nat. Hazards Earth Syst. Sci. Discuss., 2, 7409–7464, 2014
www.nat-hazards-earth-syst-sci-discuss.net/2/7409/2014/
doi:10.5194/nhessd-2-7409-2014

Natural Hazards and Earth System Sciences
Open Access
Discussions

From slope- to regional-scale shallow landslides susceptibility assessment using TRIGRS

M. Bordoni[1], **C. Meisina**[1], **R. Valentino**[2], **M. Bittelli**[3], **and S. Chersich**[1]

[1]Department of Earth and Environmental Sciences, University of Pavia, Via Ferrata 1, 27100 Pavia, Italy
[2]Department of Civil and Environmental Engineering and Architecture, University of Parma, Viale G. P. Usberti 181/A, 43100 Parma, Italy
[3]Department of Agricultural Sciences, University of Bologna, Viale Fanin 44, 40127 Bologna, Italy

Received: 24 November 2014 – Accepted: 26 November 2014 – Published: 11 December 2014

Correspondence to: M. Bordoni (massimiliano.bordoni01@universitadipavia.it)

Published by Copernicus Publications on behalf of the European Geosciences Union.

Abstract

Rainfall-induced shallow landslides are common phenomena in many parts of the world, affecting cultivations and infrastructures and causing sometimes human losses. Assessing the shallow landslides susceptibility is fundamental for land planning at different scales. This work defines a reliable methodology to extend the slope stability analysis from the local to the regional scale by using a well established physically-based model (TRIGRS-Unsaturated). The model is applied at first for a sample slope and then to the surrounding area of 13.4 km^2 in Oltrepo Pavese (Northern Italy). In order to obtain more reliable input data for the model, a long-term hydro-meteorological monitoring has been carried out at the sample slope, that has been assumed as representative of the study area. Field measurements allowed for identifying the triggering mechanism of shallow failures and were used to calibrate the model. After obtaining modelled pore water pressures at the slope scale consistent with those measured during the monitoring activity, more reliable trends have been modelled also for past landslide events, as the April 2009 event that has been assumed as benchmark. The shallow landslides susceptibility assessment obtained using TRIGRS-Unsaturated for the benchmark event appears good for both the monitored slope and the whole study area, with better results if a pedological instead of geological zoning is considered at regional scale. The scheme followed in this work allows for obtaining better results of shallow landslides susceptibility assessment in terms of reduction of overestimation of unstable areas with respect to other distributed models applied in the past.

1 Introduction

Shallow landslides can be defined as slope movements affecting a small thickness (generally lower than 2 m) of superficial deposits. The failure surface is often located along the interface between the soil and the bedrock or between soil levels with differences in permeability. These movements are very hazardous phenomena: although

NHESSD
2, 7409–7464, 2014

they generally involve small volumes of soils, as a consequence of particularly intense and concentrated rainfalls, they can be densely distributed across territories (Howard et al., 1988; Montrasio and Valentino, 2008). Moreover, these phenomena are very common in slopes close to urbanized areas and, for this reason, they can cause significant damage to cultivation, structures and infrastructures and, sometimes, human losses.

In order to assess the occurrence of rainfall-induced shallow landslides in a certain area, three main aspects can be considered of prominent importance: (1) a detailed description of the physical-mechanical triggering mechanism in relation to the site-specific characteristics of the involved soils and stratigraphy, (2) the choice of the more suited slope stability model to be applied at local scale, (3) the definition of a reliable methodology to extend the model from the local to the regional scale.

As regards the first aspect, it is well known that shallow landslide triggering mechanism is strictly linked with the hydrological and mechanical response of an usually unsaturated soil to rainfall events. In particular, the quick decrease in negative pore water pressure and the development of positive pressures when a soil approaches saturated conditions could be considered the most important cause for shallow landslide triggering (Lim et al., 1996; Vanapalli et al., 1996). Under this point of view, continuous monitoring over time of the climatic and meteorological parameters as well as the physical and hydrological properties of the unsaturated soil zone is needed to understand the triggering mechanism of shallow landslides and the main features of these phenomena. More recently, monitoring techniques have allowed focusing not only on soil hydrological and mechanical conditions during shallow landslide triggering, but also on some unsaturated soil behaviours which could play a primary role in promoting or inhibiting the development of shallow failures. In particular, several authors have paid attention to the rainwater infiltration and the groundwater fluxes in soils as well as the mechanisms of water removal from soils due to evapotranspiration and infiltration towards the underlying permeable bedrocks (Matsushi et al., 2006; Damiano et al., 2012), the time changes in the hydrological features of the soil (Matsushi and Matsukura, 2007; Dami-

NHESSD
2, 7409–7464, 2014

ano and Olivares, 2010; Askarinejad et al., 2012; Smethurst et al., 2012; Springman et al., 2013), and the increase in pore water pressure with the possible development of a perched water table in the covering soils that could promote shallow landslides (Lim et al., 1996; Simoni et al., 2004; Godt et al., 2008a, b, 2009; Baum et al., 2010, 2011). On the other hand, the trend in time of safety factor determined through classical slope stability analyses is linked to the change in time of soil hydrological parameters, especially soil pore water pressure, in relation to rainfall intensity and cumulated rainfall. This aspect is particularly important in the case of shallow failures in soils which are in unsaturated conditions before the beginning of the triggering rainfall event.

As regards the choice of the more suited method to describe the phenomena at slope scale, it depends on the objectives of the analysis: finite elements methods, for example, can be considered appropriate to analyze an area some hundreds square meters wide, but they cannot be considered suited to be applied at regional scale. Recently, physically-based models proved rather promising in assessing spatial susceptibility of shallow landslide, starting from a local slope stability analysis (Montgomery and Dietrich, 1994; Wu and Sidle, 1995; Pack et al., 1999; Iverson, 2000; Baum et al., 2002, 2008; Qiu et al., 2007; Lu and Godt, 2008; Montrasio and Valentino, 2008; Baum and Godt, 2010; Lanni et al., 2012; Rossi et al., 2013; Grelle et al., 2014), and in determining the timing and localization of shallow landslides in response to rainfall on a regional scale (Salciarini et al., 2006, 2008; Godt et al., 2008a, b; Papa et al., 2013).

At the moment, an important challenge is represented by the possibility of applying a slope stability model at different scales, providing of keeping the same level of reliability both on the single slope and on an area some square kilometres wide, with the awareness that the spatial distribution of both geotechnical and hydrological soil properties can be reasonably inferred only from a limited number of either field or laboratory tests.

The implementation of physically-based models at regional scale in respect to a single slope needs a homogenization of the soil parameters required as input data in distinct mapping units, whose boundaries can be defined in different ways. In most cases

NHESSD
2, 7409–7464, 2014

the mapping units used in distributed slope stability analyses are defined according to the geology of the bedrock (Salciarini et al., 2006; Baum et al., 2010; Sorbino et al., 2010; Rossi et al., 2013; Park et al., 2013; Zizioli et al., 2013). This choice is linked to the hypothesis that the geotechnical and hydrological properties have spatial variations due to the spatial distribution of the bedrock materials whence soils derive. More rarely, the mapping units are considered according to a pedological classification of the soil deposits (Meisina and Scarabelli, 2007) or they are defined as engineering-geological or litho-technical units on the basis of the main geotechnical and mechanical properties of the soils in an independent way with respect to the geology of the bedrock (Meisina, 2006; Grelle et al., 2014).

In this work, an attempt to define a methodology that links long-term field observations on a sample slope with the distributed slope stability analysis at regional scale is presented. In particular, the TRIGRS-Unsaturated model (Baum et al., 2008) was applied to a study area in the Oltrepò Pavese (northern Italy; Fig. 1) to assess spatial susceptibility of shallow landslides referred to a well-documented case history occurred on 27–28 April 2009 (Zizioli et al., 2013). The Oltrepò Pavese area is representative of the shallow landslides phenomena which affects the Northern Apennines sector. The study area is strongly characterized by a traditional viticulture which represents the most important branch of local economy. Due to the fact that most of shallow failures affected slopes cultivated with vineyards, it is fundamental assessing shallow landslides susceptibility for a correct land use planning, to manage agricultural best practices and to reduce the economical effects of these landslides. The Oltrepò Pavese area is representative of the shallow landslides phenomena which affects the Northern Apennines sector. However, The developed methodology may be applied in other geological contexts where vineyards are located on slopes affected by shallow landslides (Tiranti and Rabuffetti, 2010; Galve et al., 2014).

The main goals of the work were: (i) to identify the hydrological behaviour of the slope soils in the study area through a continuous field monitoring on a sample slope, (ii) using field data to calibrate the TRIGRS-Unsaturated model, (iii) to evaluate the effi-

NHESSD
2, 7409–7464, 2014

ciency of the TRIGRS-Unsaturated model on the estimation of the pore water pressure trend at slope scale, (iii) to compare results of the TRIGRS-Unsaturated distributed analyses at regional scale in the study area taking into account different unit mapping of the slope soils.

2 The study area

The study area is located in the north-eastern sector of Oltrepò Pavese which belongs to the north-western Italian Apennines (Fig. 1). The area is 13.4 km^2 wide and is characterized by the presence of vineyards, which constitute the 55 % of the land cover, shrublands (30 %) and woodlands (15 %) that correspond to vineyards abandoned after the 1980s.

The slopes are characterized by a medium-high gradient, with slope angle that can reach 35°, which sometimes descend to small narrow valley formed by creeks. The slope elevation ranges from 85 to 350 m a.s.l.

The climatic regime is typical of continental areas, with a mean annual temperature of 12 °C. Considering recent rainfall data available from 2004 to 2013 coming from a weather station located closely near the study area at a similar elevation (Canevino rain-gauge station, ARPA Lombardia monitoring network), the mean yearly rainfall amount of the period 2004–2013 was 634.3 mm, with the rainfall amounts which tend to distribute in less but more intense events (Alpert et al., 2002), thus favouring slope instability, as already observed in other environmental contexts (Schnellmann et al., 2010).

In this area, the bedrock is characterized by a series of formations belonging to the Mio-Pliocenic succession that geologically characterizes this Apennine area and is called “Serie del Margine” (Vercesi and Scagni, 1984). It is constituted of continental deposits, in particular sand, sandstones and conglomerates, belonging to Rocca Ticozzi Conglomerates (R. T. Cong.) and Monte Arzolo Sandstones (M. A. Sand.). These bedrock levels alternate with marine deposits, especially marls and sandy marls,

NHESSD
2, 7409–7464, 2014

called “Sant’Agata Fossili Marls” (S. F. Marls), and evaporitic deposits, chalky marls, gypsum, belonging to Gessoso-Solfifera Formation (G. F. Form.) (Fig. 2a). The bedrock strata dip mainly east-northeast with moderate inclinations.

In this sector of the Oltrepò Pavese, the shallow soils mainly derive from the bedrock weathering and have a prevalently clayey-silt or silty-sand texture. The soil thickness, determined in different points of this area through trench and manual pits (Zizioli et al., 2013), ranges between a few centimetres to 2.5 m and it generally increases from the top to the bottom of the slopes, also due to the presence of landslide accumulation areas.

The soils have been also classified by the pedological point of view and this information is available from the soil maps at a scale of 1 : 10 000 covering the entire study area (ERSAL, 2001). Four pedological units can be identified (Fig. 2b):

- BRS1: Eutric Leptosols characterized by well drainage, thickness between 0.3 and more than 2.0 m, high carbonate content (> 20 %) and parent material composed by marls, sandy marls and marly sands;
- FGE1: Calcaric Cambisols characterized by well drainage, thickness that can reach values higher than 1.5 m, high carbonate content (> 20 %) and parent material composed by marls and evaporitic deposits (Gessoso-Solfifera Formation);
- ILM1/RUM1: Eutric Leptosols characterized by very well drainage, thickness lower than 1.5 m, low carbonate content (< 10 %) and parent material composed by sandstones, conglomerates, sandy marls;
- MRL1: Calcaric Cambisol characterized by well drainage, thickness higher than 0.8 m, medium carbonate content (between 10 and 20 %) increasing with and parent material composed by sandstone and lenses of conglomerates.

FGE1 pedological unit seems to be present only where the bedrock is constituted by the deposits of the Gessoso-Solfifera Formation, while the other ones are widespread also for different geological formations.

NHESSD
2, 7409–7464, 2014

The study area is characterized by a high density of landslides: the IFFI (Italian Landslides Inventory) database indicates the presence of several deep landslides with failure surfaces below 2–3 m from ground level. In particular, these phenomena are rotational slides, translational slides and complex landslides (roto-translational slides evolving in earth flows) (Cruden and Varnes, 1996) and do not show evidence of recent movement, so they can be classified as dormant landslides. These phenomena were triggered by prolonged rainfall without significantly high intensity.

The widespread shallow landslides occurred on 27–28 April 2009 constituted the first documented case of a rainfall-induced shallow landslide event that had hit the Oltrepò Pavese since the 1950s. Throughout the area of Oltrepò Pavese, this event caused the triggering of more than 1600 shallow landslides (Zizioli et al., 2013): the highest density was registered in the study area (491 landslides, about 36 landslides per km^2). Shallow landslides were triggered due to an extreme rainfall event characterized by 160 mm of cumulated rain in 62 h with a maximum intensity of 22 mm h^{-1} at 21:00 LT on 27 April (Zizioli et al., 2013). This event provoked fatalities and damage to/blocking of roads in several places (Zizioli et al., 2013).

Further shallow-landslide events occurred in the study area in the period between March and April 2013 (Zizioli et al., 2014) and between 28 February and 2 March 2014. These events caused the triggering of a limited number of shallow landslides (17 and 20 respectively) in the study area.

Rainfall-induced shallow landslides identified in the study area tended to be concentrated in three main geomorphological contexts: (i) at the top of steep slopes (slope angles > 15–20°) with continuous profiles, (ii) corresponding to a slope angle change, from a gentle slope to a steep slope, (iii) in morphological jugs that break the continuity of the slopes. In these areas, the greater superficial runoff and the convergence of sub-superficial outflows in the cover materials promote the increase in pore water pressure and the saturation of the covering soils. These geomorphological frameworks that promote the development of shallow failure source areas were already highlighted in

NHESSD
2, 7409–7464, 2014

other contexts where rainfall-induced shallow landslide events were triggered (Crosta and Frattini, 2003; D'Amato Avanzi et al., 2004; Dapporto et al., 2005).

According to Cruden and Varnes' (1996) and Campus et al.'s (1998) classifications for rainfall-triggered shallow landslides, four main types of landslide were recognized (Fig. 3): (a) incipient translational slides, where fractures are present but the displaced mass has limited movement with little internal deformation (Fig. 3a), (b) translational soil slides, where the mass has moved, the failure surface is completely exposed and the collapsed materials breaks into different blocks (Fig. 3b), (c) complex landslides when they start as shallow rotational-translational failures and then evolve into earth-flow due to the high amount of water and the fabric loss of collapsed materials (Fig. 3c), (d) disintegrating soil slips, similar to type (c) but in which the accumulation zone is not recognizable because the collapsed materials are completely dispersed along the slope and at its toe (Fig. 3d). Type (c) and type (d) shallow landslides were usually predominant in the events that affected this area.

Shallow landslides mainly affected the superficial soils above the weathered or not-weathered bedrock and the failure surfaces are located in correspondence with the contact between the soil and the bedrock, ranging between 0.5 and 2.0 m from ground level. More rarely, these phenomena have failure surfaces located at the point of contact with the soil levels with differences in permeability. These movements mainly occurred in vineyards and uncultivated slopes where shrubs and grass are prevalent. In contrast, a significant number of landslides involved woodland formed by trees which had developed in the last 30 years on abandoned vineyards.

NHESSD
2, 7409–7464, 2014

3 Materials and methods

3.1 Soil characterization and monitoring of the field hydrological conditions

In the study area, an integrated hydro-meteorological monitoring station has been installed since 27 March 2012 in a test-site slope located near the village of Montuè (municipality of Canneto Pavese; Fig. 1).

The slope is characterized by a medium-high topographic gradient (between 22 and 35°). It has an E–W orientation and an altitude ranging from 210 to 175 m a.s.l. This test-site was subjected to shallow landslides in the near past and, for its geological and morphological characteristics, can be considered representative of the whole study area.

A multidisciplinary characterization of the monitored test-site slope was carried out. The representative soil of the slope is 1.3 m thick. The soil belongs to the ILM1/RUM1 pedological unit. Between 1.1 and 1.3 m from ground, the soil is characterized by the presence of a calcic horizon (Cgk), labelled as G in Fig. 5, enriched in carbonate concretions and with amount of carbonate of 35.3 %. The soil has a basic pH (around 8.3–8.8), a low organic carbon content (O.C., less than 3.0 %) and a steady cationic exchange capacity (C.E.C., 12.3–15.9 meq L^{-1}) along depth.

The geotechnical characterization of the slope deposits was based on standard soil analyses carried out according to the ASTM (American Society for Testing and Materials) standards. The performed tests included (i) assessment of the physical parameters of materials (grain size distribution, bulk densitiy, Atterberg limits) and (ii) triaxial tests which allowed the determination of shear strength parameters in terms of effective stresses.

The soil derived from weathering of sands and poorly cemented conglomerates belonging to Rocca Ticozzi Conglomerates. Different soil horizons of the slope have a clayey sandy silt texture, with high silt amount, ranging from 51.1 to 65.6 %, clay content between 21.3 and 29.0 % and different amount of gravel and sand (Table 1). By analyzing the clay soil fraction (< 2 µm) through X-ray diffraction tests it mostly appears

NHESSD
2, 7409–7464, 2014

constituted by smectite and chlorite. In particular, smectite constitutes about 50 % of the soil finest fraction, and then, about 10–15 % of the solid particles of the studied soils. The weathered bedrock at 1.4 m from ground, labelled as We. Bed. in Fig. 5, is constituted of a sand lens with a sand amount of 75.0 % (Table 1).

Acco rding to the USCS classification, soil horizons are prevalently non-plastic or slightly plastic (CL). The liquid limit (w_L) ranges from 38.5 to 41.9 %, while the plasticity index (P_I) ranges from 14.3 to 17.1 % and both remain steady along the depth (Table 1). The unit weight (γ) increases between 0.6 and 1.0 m below the ground level from 16.7 to 18.6 kN m^{-3} and then keeps rather steady with depth (Table 1).

Peak shear strength parameters were reconstructed at different depths through triaxial tests. Till 1.0 m from ground, the soil horizons have friction angle (φ') between 31 and 33° and nil effective cohesion (c') (Table 1). At 1.2 m from ground, the soil level is characterized by a friction angle equal to 26° and effective cohesion of 29 kPa (Table 1).

Hydrological properties of different soil horizons were determined through laboratory reconstruction of the Soil Water Characteristic Curve (SWCC) and the Hydraulic Conductivity Function (HCF). These functions were reconstructed through a combination of a Wind Schindler Method (WSM; Schindler, 1980; Peters and Durner, 2008) technique (Hyprop, UMS GmbH, Munich, Germany) with a Vapour Pressure Method (VPM; Rawlins and Campbell, 1986) device (WP4T, Decagon Devices, Pullman, WA) on undisturbed soil samples. The experimental data were fitted through the Van Genuchten (1980) and Mualem (1976) models. The parameters of these models (saturated water content θ_s, residual water content θ_r, fitting parameters α and n, saturated hydraulic conductivity K_s) were then estimated using the Marquardt (1963) algorithm. All the soil levels have similar values of α (0.007–0.013 kPa^{-1}) and θ_r (0.01–0.03 m^3 m^{-3}). The n and θ_s parameters are slightly higher till 0.6 m from ground with respect to the deeper levels. Moreover, K_s is quite steady around 1.0 and 2.5 × 10^{-6} m s^{-1}, except for the soil level at 1.2 m from ground which is less permeable (0.5 × 10^{-6} m s^{-1}; Table 2).

A detailed description of the monitoring station is reported elsewhere (Bordoni et al., 2014; Fig. 4). In this paper, the necessary information required for completeness are

NHESSD
2, 7409–7464, 2014

provided. The station allows to collect data with a time resolution of 10 min. The following meteorological parameters are measured: rainfall depth, air temperature, air humidity, atmospheric pressure, net solar radiation, wind speed and direction. Some probes are installed in the soil and in the weathered bedrock at different depths to measure soil water content and soil pore water pressure. In particular, six time domain reflectometer (TDR) probes were installed at 0.2, 0.4, 0.6, 1.0, 1.2, 1.4 m from ground level to measure the soil water content, while a combination of three tensiometers and three heat dissipation (HD) sensors installed at depths of 0.2, 0.6, 1.2 m allows for measuring soil pore water pressure. HD sensors allow only pore water pressure lower than -10^1 kPa (Bittelli et al., 2012) to be acquired; thus tensiometers are installed in correspondence of the HD sensors to measure pore water pressure in the range above -10^1 kPa.

The monitoring equipment allows to identify the main soil hydrological behaviours, in particular the soil response to the different seasonal rainy conditions and to various rainfall intensities. The test-site slope can represent in a good way the geotechnical and hydrological features of the slopes affected by shallow landslides in the whole study area. For this reason, the data from the continuous monitoring on the sample slope can be useful to identify the soil hydrological conditions which can lead to the triggering mechanism of the shallow landslides in similar conditions. The field data can be used to infer the soil conditions for periods without monitoring in order to evaluate the prediction skill of a physically based model such as TRIGRS-Unsaturated, used for shallow landslides susceptibility at regional scale.

3.2 Homogenization of the soil parameters in the study area

To assess shallow landslides susceptibility using physically-based models it is fundamental the distribution of the main geotechnical and hydrological properties required as input parameters to obtain the trend of the slope safety factor (Fs) in time. But passing from the site scale, where detailed field and laboratory test results can be available, to a regional scale, where data can be available only for a limited number of sites, it

NHESSD
2, 7409–7464, 2014

appears important to establish which kind of characteristics ought to be considered "constant" to assume the available data as representative.

In order to guess an answer to this question, the implementation of TRIGRS model in the study area was made by using different types of unit mapping (geological and pedological), whose class distribution across the study area is represented in Fig. 3.

The main geotechnical and mechanical soil properties were assigned to each unit after performing an averaging procedure of the data collected through laboratory tests on 160 soil samples taken in different sites in the study area. As observed in the monitored slope, no significant changes in geotechnical properties, in particular for grain size distribution and Atterberg limits, are identified along the depth in soil levels.

The main differences between the classes for each unit mapping type are linked to the grain-size distribution. In fact, the geological and the pedological units can be distinguished on the basis of the sand and clay amounts. The soils derived from the weathering of Monte Arzolo Sandstones and Rocca Ticozzi Conglomerates were classified as clayey-sandy-silt because the amount of sand is generally more than 15 % (Table 3). Instead, the soils derived from the weathering of the Sant'Agata Fossili Marls and Gessoso-Solfifera Formation were classified as clayey-silt due to a sand amount generally lower than 10 % and the prevalent silt content (Table 3). Moreover, the soils derived from weathering of Gessoso-Solfifera formation have a clay amount (37.1 %) significantly higher than the other units (Table 3). The BRS1 and MRL1 pedological units group soils with clayey silt texture (Table 3), while ILM1/RUM1 soils are clayey-sandy-silt due to a mean sand content of 19.3 %. Instead, FGE1 class has soils with a clayey-silty texture due to similar mean values of silt and clay content (respectively 46.9 and 43.3 %; Table 3).

According to the USCS classification, the majority of the classes in all the unit mapping groups non-plastic or slightly plastic soils (CL), with a mean liquid limit w_L that ranges between 39.7 and 43.9 %, and a mean plasticity index P_I that ranges between 18.1 and 22.7 % (Table 3). Only FGE1 pedological class presents high plastic soils (CH) with a mean w_L of 52.4 % and a mean P_I of 31.8 % (Table 3).

NHESSD
2, 7409–7464, 2014

The soil unit weight γ is similar between the different classes for each unit mapping (Tables 1–3): the mean values range between 17.0 and 18.1 kN m^{-3}. Furthermore, also the shear strength parameters of the soils, i.e. the peak friction angle φ' and the effective cohesion c', are quite similar for all the considered soils (Table 3). In particular, φ' ranges between 24 and 27°, while c' keeps between 1.2 and 2.0 kPa.

A similar procedure has been carried out in order to assign the hydrological parameters (in terms of Soil Water Characteristic Curve – SWCC) to the different selected units. In particular, the Rosetta pedotransfer function model (Schaap et al., 2001) was applied to the grain size distribution of the soil samples to determine the parameters of SWCCs and of HCFs of the materials of each identified class according to the models of Mualem and Van Genuchten (Table 4). The average values of Mualem and Van Genuchten models parameters (θ_s, θ_r, α, n, K_s) are very similar between the classes (Table 4).

The WRCs and HCFs were also reconstructed for eight undisturbed samples taken in the study area through the same methods (WSM and VPM) used for the soil samples of the monitored slope. For these soils, the reconstructed Mualem and Van Genuchten models parameters are confident with respect to the values modelled through Rosetta pedotransfer function for θ_s, α, n and K_s: in fact, the percentage of mean error (E_r) ranges between 2.3 and 9.9 % (Fig. 5a, c–e). Only θ_r values modelled through Rosetta are quite higher than the measured values through Hyprop technique (E_r = 50.1 %, Fig. 5b). Instead, this error is not so big considering the low values which characterize the studied soil (e.g. measured θ_r of 0.02 m^3 m^{-3} against an estimated θ_r of 0.04 m^3 m^{-3}).

This aspect confirms the reliability of modelling the soil hydrological properties in the study area through the Rosetta model, allowing for correctly identifying the mean values of these properties to be assigned to the selected classes of the unit mapping.

NHESSD
2, 7409–7464, 2014

3.3 The TRIGRS-Unsaturated model

The TRIGRS-Unsaturated model (Baum et al., 2008) is a Fortran program designed for modelling the timing and distribution of rainfall-induced shallow landslides (Baum et al., 2010; Liao et al., 2010; Sorbino et al., 2010; Park et al., 2013; Zizioli et al., 2013a). This physically-based model considers the method outlined by Iverson (2000) to explain shallow landslide triggering in relation to rainwater infiltration, with the implementation of complex storm histories, assuming an impermeable basal boundary at a finite depth, and a simple runoff-routing scheme. This model computes the pore water pressure and Fs during different moments of a rainfall event that could have durations ranging from hours to a few days, identifying, in particular, the changes in the pore water pressure and in the Fs due to rainwater infiltration.

The model allows for taking into account the unsaturated conditions of the soils at the initial stage through the simple analytic solution for transient unsaturated infiltration proposed by Srivastava and Yeh (1991). The program models pore water pressure changes using analytical solutions for partial differential equations that represent one-dimensional vertical flow, considering the propagation of the flow into an isotropic, homogeneous material for either saturated or unsaturated conditions, according to Iverson's model (Baum et al., 2002, 2008).

In order to model the soil hydrological pattern for rainwater infiltration, TRIGRS-Unsaturated requires soil hydrological properties as input parameters. In particular, besides the saturated hydraulic conductivity K_s, the saturated water content θ_s and the residual one θ_r; it is also required a fitting parameter indicated as α_G that represents the fitting parameter of Gardner's (1958) SWCC fitting equation.

The use of step-function series allows TRIGRS-Unsaturated to represent pore water pressure changes due to variable rainfall intensity input during the considered event, and a simple runoff-routing model allows for the diversion of excess water from impervious areas to more permeable downslope areas.

NHESSD
2, 7409–7464, 2014

An infinite slope model is coupled with the hydrological model to compute the Fs of a slope. In this case, the Fs at different time instants in different points and depths of the analyzed area ($F_s(z,t)$) is calculated both in unsaturated and saturated conditions, also considering its change over time during the studied rainfall event, due to the rise in pore water pressure $\psi(z,t)$, through Eq. (1):

$$F_s(z,t) = \frac{\tan\phi'}{\tan\beta} + \frac{c' - \psi(z,t)\gamma_w \tan\phi'}{\gamma z \sin\beta\cos\beta} \quad (1)$$

where φ' is the soil friction angle, c' is the effective cohesion, γ_w is the unit weight of the water, β is the slope angle, γ is the unit weight of the soil and z is the depth below the ground level in which a potential sliding surface could develop.

The TRIGRS-Unsaturated model has been applied to different rainfall events measured by the monitoring station installed in the study area during its activity. The modelled pore water pressures at two depths, 0.6 and 1.2 m from ground, for each considered rainfall in correspondence of the monitored slope were then compared with values measured during the same rainfall at the monitoring station. The goodness of TRIGRS-Unsaturated model on pore water pressure modelling was evaluated with the Root Mean Square Error (RMSE) statistical index, expressed in Eq. (2) as:

$$\mathrm{RMSE} = \sqrt{\frac{\sum_{i=1}^{n}(\psi_{o,i} - \psi_{m,i})^2}{n}} \quad (2)$$

where ψ_o is the observed water pore water pressure, ψ_m is the pore water pressure estimated by the model, n is the number of observations. The more the value of RMSE approaches 0 kPa, the more the prediction model is effective and accurate.

Moreover, TRIGRS-Unsaturated was applied considering the benchmark rainfall event of 27–28 April 2009 for the assessment of shallow landslides susceptibility and taking into account the two different types of unit mapping (geological and pedological). The predictive capability of the reconstructed models has been evaluated through

NHESSD
2, 7409–7464, 2014

two indexes called “Success Index” (SI) and “Error Index” (EI), respectively (Sorbino et al., 2007, 2010). The SI is the ratio (in percentage) between the number of elementary DEM (Digital Elevation Model) cells occupied by shallow landslides and the number of elementary cells computed as unstable (safety factor < 1.0) by the model. Instead, the EI represents the ratio (in percentage) between the number of elementary cells computed as unstable, which do not correspond to observed shallow landslides, and the number of elementary cells of the study area not affected by phenomena and, then, consider as stable (safety factor > 1.0).

The results of the reconstructions through TRIGRS-Unsaturated model were also compared, in terms of SI and EI, with the results obtained in a previous work through TRIGRS-Saturated (Baum et al., 2002), SINMAP (Pack et al., 1999) and SLIP (Montrasio and Valentino, 2008) models in the same study area and for the same event, by Zizioli et al. (2013).

4 Results

4.1 Monitored soil and weathered bedrock hydrological behaviours

As reported in the introduction, the first step to appropriately model rainfall-induced landslides both at slope and regional scale is a detailed description of the physical-mechanical triggering mechanism in relation to the site-specific characteristics of the involved soils and stratigraphy. Data from the monitoring station were used to determine the dynamics of soil water content and soil pore water pressure at the test site, in relation with the characteristics of the different soil levels and the weathered bedrock (Fig. 6). The monitored hydrological behaviours can represent in a good way the typical conditions that characterize the surrounding study area. In this work, the period between 27 March 2012 and 1 October 2014 was analyzed.

Average hourly values of water content and pore water pressure were considered. Due to break of the tensiometer at 0.2 m from ground level, at this depth pore wa-

NHESSD
2, 7409–7464, 2014

ter pressure in the range between 0 and -10^1 kPa was not measured since November 2012 till the end of the analyzed period. No data were acquired between 10 and 15 January 2014 due to a not correct functioning of the station alimentation system.

In the analyzed period, the water content ranged between 0.10 and 0.45 $m^3 m^{-3}$ in the topsoil, and between 0.15 and 0.38 $m^3 m^{-3}$ in the weathered bedrock. Instead, pore water pressure ranged from positive values, till 12.7 kPa in G horizon, to values in the order of -10^3 kPa.

The installed tensiometers require a correction of the measured values due to height of the water present in the column of the instrument, with an increase of 1 kPa for each 0.1 m of depth in the soil. For this reason, it is possible to measure also positive values of the pore water pressure, as already shown also in previous works (Zhan et al., 2006).

By analyzing the data acquired along two years monitoring, it is immediately clear that water content and pore water pressure dynamics are strictly connected to rainfall trends and that different hydrological behaviours can be identified in the soil profile (Fig. 6).

The soil horizons till 0.6–0.7 m from ground level had a faster response than the deepest soil horizons to long dry or long wet periods. In summer months, decreases of the water content and of the pore water pressure are faster in the most shallow soil horizons than in the deeper ones (Fig. 6), due to evapotranspiration effects and to the water uptake from the roots of grass and shrubs. Changes in hydrological parameters are not as rapid in soil levels deeper than 0.6–0.7 m from ground and in weathered bedrock (Fig. 6): this different behaviour is linked to the fact that these levels are less affected by evapotranspiration and roots zone effects. During rather prolonged rainy periods following dry periods, as in autumn months, re-wetting of shallowest soil horizons is fast (Fig. 6), as well as after rainfall events characterized by low duration and low cumulative rainfall (e.g. 34.8 mm in 21 h on 31 October–1 November 2012; 42.2 mm in 34 h on 6–7 October 2013). On the other hand, re-wetting of soil horizons deeper than 0.6–0.7 m from ground level as well as of the weathered bedrock is not so fast and only prolonged rainy periods, with many rainfall events in few days or weeks, can provoke

NHESSD
2, 7409–7464, 2014

an increase of the pore water pressure and of the water content in correspondence of this level (Fig. 6).

The rapid re-wetting as consequence of early autumn rainfalls of the soil horizons till 0.6–0.7 m and the abrupt increase in pore water pressure in a time span of 5–10 h after the start of the rain during summer concentrated events, as it occurred on 27 June 2013 (13.3 mm in 2 h), on 26 August 2013 (16.5 mm in 3 h), and on 11 September 2013 (9.1 mm in 3 h), may also be due to the presence of desiccation cracks and other macro-voids all along the soil profile, where preferentially rainwater could flow. This fact could promote a quick development towards near saturated conditions of the cracks and the macro-voids (Bittelli et al., 2012; Smethurst et al., 2012).

In winter and spring months, especially between December and May, frequent precipitations can increase the soil wetness till it approaches or reaches saturated conditions (Figs. 6 and 7). Soil water content ranges between 0.38 and 0.45 $m^3 m^{-3}$. Instead, pore water pressure keeps steady between −7 and −3 kPa in soil horizons till 0.6 m from ground, while completely saturated conditions were reached in the G horizon at 1.2 m from ground as testified by the values of pore water pressure which kept quite steady around 0 kPa (Fig. 7) till reaching positive values around 1–3 kPa in correspondence of more intense rainfall events (e.g. 29.8 mm in 24 h in 24–25 March 2013; 24.6 mm in 15 h in 30 March 2013; 29.5 mm in 26 h in 4–5 April 2013; 34.6 mm in 44 h in 18–20 January 2014; 68.9 mm in 42 h in 28 February–2 March 2014). Thus, in this situation a moderately intense rainfall could not cause a further increase of pore water pressure and water content (Figs. 6 and 7).

During wet periods, water content in the weathered bedrock at 1.4 m from ground was lower than the overlying G horizon (Fig. 6a).

According to the monitored data, it could be supposed that during winter and spring months a perched water table can form in the test-site slope soils and it keeps steady at 1.2 m from ground till the end of the spring. The thickness of this water table is of about 0.1 m over the contact between the soil and the weathered bedrock. Also when no rain falls for many days, as between 5 and 21 March 2014 (Fig. 7), pore water pressure

NHESSD
2, 7409–7464, 2014

keeps steady in positive values range at this depth, thus confirming the presence of the perched water table. Instead, in correspondence of particularly intense rainfalls, water table can grow up to 0.8–1.0 m, as testified by the significant increase in water content at 1.0 m from ground till conditions of complete saturation are attained (water content between 0.39 and 0.42 $m^3 m^{-3}$).

This condition was not noticed in correspondence of other rainfall events in wetting periods during the monitored time span. In correspondence of this situation a shallow landslide affected the test-site slope (Fig. 7). For this reason, the triggering mechanism of rainfall-induced shallow landslides in the study area could be due to the uprising of a thin (0.1–0.2 m) perched water table present in winter and spring months in the slope soils of the study area in correspondence of particularly intense rainfalls. Thus, it is fundamental taking into account this mechanism on modelling shallow landslides susceptibility through physically-based models.

Soil–atmosphere interaction phenomena observed during wetting periods were considered as a good benchmark for the application of the TRIGRS-Unsaturated model. In fact, the model allows for modelling shallow landslides triggering due to the uprising of a perched water table (Baum et al., 2008), as we can observe in the monitored test-site. This fact implies that the lowest computed safety factors correspond to areas characterized by the presence of a natural permeability barrier, such as the soil-weathered bedrock contact, where shallow landslides sliding surface develops, as it is possible to observe in the study area (Zizioli et al., 2013).

4.2 TRIGRS-Unsaturated model implementation

A Digital Elevation Model (DEM) acquired before the April 2009 event with a grid size of 10 m × 10 m provides the topographic basis for the study area reported in Fig. 1. In correspondence of the monitored slope, TRIGRS-Unsaturated model was also applied considering a more detailed DEM, with a grid size of 2 m × 2 m on an area of about 3290 m^2.

NHESSD
2, 7409–7464, 2014

TRIGRS-Unsaturated was implemented considering both the DEMs in order to evaluate also the differences on modelling passing from slope scale and high resolution to a regional scale with lower resolution.

For analyzing the role played by the type of unit mapping, the study area was divided into different regions according to each zoning. All input data were acquired from a GIS database in a "raster" form. For each unit mapping, a map was generated at the same spatial resolution of the DEM.

The soil geotechnical and hydrological parameters required as input data by TRIGRS-Unsaturated are summarized in Table 5. The unit weight γ, the friction angle φ' and the cohesion c' correspond to the average values of each unit reported in Table 3, as well as for the saturated and residual water content θ_s and θ_r and the saturated hydraulic conductivity K_s, whose values are summarized in Table 4. On the basis of the characteristic values of K_s of each class, we obtained the values of soil hydraulic diffusivity D_0 required in the model, estimated in accordance with Baum et al. (2011) to be $\sim 2 \times K_s$ (Table 5).

TRIGRS-Unsaturated model required also a parameter indicated as α_G which corresponds to the fitting parameter of Gardner's (1958) model for SWCC. Parameter α_G has been estimated on the basis of the α and the n fitting parameters of Van Genuchten's model, as reconstructed for each unit through the method proposed by Ghezzehei et al. (2007) and expressed in Eq. (3):

$$\alpha_G = \alpha(1.3n). \quad (3)$$

Slope angle and flow direction maps required by the TopoIndex (Topographic Index) utility were derived from the considered DEM using SAGA Gis (version 2.0.8; Conrad, 2006). By assuming that the gradient of the slope angle is rather uniform along each hillslope on the study area and that it is almost regular – slightly convex in shape – a slope proportional weighting factor (exponent = 1 in TopoIndex) has been chosen for the runoff distribution. This scheme distributes the flow excess to all adjacent downslope cells with a weighting factor proportional to the slope (Baum et al., 2008).

NHESSD
2, 7409–7464, 2014

To create a continuous map of topsoil thickness, a geomorphologically indexed model, based on the local slope angle, the elevation and the topographic position, was used (Zizioli et al., 2013).

An analysis of the reliability of pore water pressure at different depths, modelled by TRIGRS-Unsaturated, was performed. In correspondence of the monitoring station and of the most intense rainfall events of the wet periods of the monitored time span (23–25 March 2013, 30 March 2013, 4–5 April 2013, 20–22 April 2013, 18–20 January 2014, 28 February–2 March 2014; Table 6), the measured values of pore water pressure measured at 0.6 and 1.2 m from ground level were compared to the modelled pore water pressure values using TRIGRS-Unsaturated.

For these analyses, the initial water table depth across the study area was chosen according to the information obtained during the monitoring time span in the test-site slope. The most superficial measured pore water pressure values (till 0.6 m from ground) were considered representative of the hydrological conditions in the selected area and were used to estimate the water table depth according to Eq. (4) (Comegna, 2008):

$$d = \frac{\psi_g}{\gamma_w \cos^2 \beta} \quad (4)$$

where ψ_g is the pore water pressure near the ground surface, d is the water table depth, β is the slope angle and γ_w is the unit weight of water.

As regards the data related to the rainfall events, hourly values from the datalogger of the monitoring station were included in the model (Table 6).

The modelling of pore water pressure for 2013–2014 monitored rainfalls was made considering the soil geotechnical and hydrological data reported in Table 5. In particular, for the monitoring station area the geological class is Rocca Ticozzi Conglomerates and the pedological class is ILM1/RUM1.

Moreover, for the event occurred on 27–28 April 2009, the hourly rainfall intensities recorded by the Cigognola rain gauge during this event were assumed as rainfall input

NHESSD
2, 7409–7464, 2014

data (Table 6). For these analyses, on the basis of what observed at the monitoring station during winters and springs, it was assumed that a thin perched water table was already present in the extended study area before the beginning of the event. It was also assumed that this water table had an upper limit located at about 0.1 m above soil-bedrock contact and a parallel trend with respect to this contact.

4.3 Comparison between measured and estimated pore water pressure

Figures 8 and 9 show the comparison between measured and modelled pore water pressure trends at 0.6 and 1.2 m, respectively, for the considered rainfall events reported in Table 6. The modelled trends for the test-site soil are the same even considering the two different unit mapping types, because the soil hydrological properties keep constant (Table 5). Moreover, the same trends of estimated pore water pressure were found considering the analyses with the two used DEMs.

The graphs related to the pore pressure trends show how TRIGRS-Unsaturated is able to adequately model the increase in pore pressure during a rainfall event.

In particular, differences greater than 2 kPa between the measured and estimated values have never been found at both depths, except for the final phase of the 28 February–2 March 2014 event. This can be deemed a very positive result, especially considering that the tensiometers used in the monitoring are characterized by an accuracy equal to ±1.5 kPa.

The lowest RMSEs were found for shorter events and in correspondence of 1.2 m more than at shallow investigated depths (Table 8). Generally, RMSEs values are lower than 1.5 kPa for all the considered events and at 1.2 m from ground they are always lower than at 0.6 m (Tables 7 and 8). The differences between modelled trends at different depths can be linked to the different hydrological properties of soil horizons. Overall, the trends in increasing pressures agree with each other. The authors of the original code (Baum et al., 2002, 2008) pointed out that TRIGRS was developed to model intense weather events and not long periods with low levels of precipitation.

NHESSD
2, 7409–7464, 2014

It is possible noting that for the rainfall events occurred on 23–25 March 2013, 30 March 2013 and 4–5 April 2013 a sudden increase in the pore water pressure during the first stages of each rainfall event, as modelled by TRIGRS-Unsaturated, is clearly visible at 1.2 m from ground (Fig. 10a–c). In particular, the field measurements show a quite negative trend in pore water pressure while the model shows a slightly positive increase.

Furthermore, TRIGRS-Unsaturated models for each event the highest pore water pressure value at the end of the rainfall, while in many cases (in particular for the event occurred on 28 February–2 March 2014) field measurements show that the highest values of pore water pressure are not reached at the end of the event (Figs. 8f and 9f). It is important noting that for these rainfall events the Fs modelled by TRIGRS-Unsaturated kept always over 1.0 (stable conditions). In fact, no shallow landslide were detected after these events next to the monitoring station.

Pore water pressure trends were also modelled for the April 2009 event (Fig. 10), when field measurements were not available and many shallow landslides occurred in the area. For the test-site slope, TRIGRS-Unsaturated registered the greatest increase in pore water pressure at 0.6 and 1.2 m around the peak intensities of the event. In particular, at 1.2 m, pore water pressure reached about 6 kPa at 02:00 LT on 28 April 2009 and remained constant until the end of the event (Fig. 10). Most of landslides triggered between the late evening of 27 April and the early hours of 28 April (hourly interval 32–48 in the plot of Fig. 11).

Although, in this case, a comparison with field measurements is not possible, due to the lack of field data, this result can be considered reliable, also accounting for the presence of a perched water table at 1.2 m from ground (positive pore water pressure; Fig. 10) at the beginning of the event, which is the typical condition also observed in the test-site slope during wet months.

NHESSD
2, 7409–7464, 2014

4.4 Shallow landslides susceptibility assessment at different scales

Figure 11 shows the shallow landslides susceptibility scenario referred to April 2009 in correspondence of the monitored test-site slope considering the DEM with the grid size of 2 m × 2 m. The figure refers to the period when shallow landslides triggered (between 32 and 48 h since the beginning of the rainfall): after this time span, the scenarios keep steady, following the trend of modelled pore water pressure (Fig. 10).

The results were the same considering as mapping either a geological or a pedological zoning. The assessment of shallow landslides susceptibility at slope scale seemed satisfactory: for the DEM with grid size of 2 m × 2 m, the shallow landslides scarps fell in areas modelled by TRIGRS-Unsaturated as unstable, even if there was an overestimation of the unstable areas all over the slope (Fig. 11). The satisfactory result at slope scale, in terms of comparison between modelled and really occurred landslides, confirms the reliability of the calibration methodology.

Figure 12 shows the shallow landslides susceptibility scenarios referred to April 2009 event for the whole study area, by taking into account the selected types of unit mapping. In order to quantify the differences between the model results based on different unit mapping, SI and EI indexes were computed from the Fs output maps of the study area. Generally, the two scenarios did not provide a significant overestimation of the unstable areas: the maps have similar EI values, ranging between 10.1 and 10.2 % (Fig. 13). The differences between the obtained maps become evident considering the SI values: the best prediction of the effective unstable areas was obtained considering the pedological unit mapping (78.9 %) in respect to the scenarios obtained through geological unit mapping, which has a SI index of 73.3 % (Fig. 13).

The results obtained through the TRIGRS-Unsaturated model have also been compared with the results obtained, for the same area, by Zizioli et al. (2013) using TRIGRS-Saturated, SINMAP and SLIP models (Fig. 14). These three models were applied considering different initial hydrological conditions with respect to those considered in this work (Zizioli et al., 2013). Based on the same unit mapping (geological zon-

NHESSD
2, 7409–7464, 2014

ing), TRIGRS-Unsaturated model provided a better susceptibility assessment in terms of ratio between SI and EI in respect to the other models. In fact, SLIP and SINMAP models have similar SI (71.7–72.4 %) and EI (30.3–32.2 %), which denote a significant overestimation of the unstable areas, while TRIGRS-Saturated has a lower EI, ranging between 10.0 and 10.2 %. TRIGRS-Unsaturated scenario models slightly better the effective unstable areas, as testified by the highest SI value (73.3 %; Fig. 14).

5 Discussion and conclusions

In this work, the implementation of a slope stability model for rainfall-induced shallow landslides assessment has been presented. The followed work procedure allowed to keep the same level of reliability at different scales, both on a single slope and on an area some square kilometres wide in the Oltrepò Pavese (Northern Italy).

The work procedure consists in the identification of a sample slope in an area of some square kilometres which can be assumed as representative of the whole area.

Field measurements from a monitoring station installed on the sample slope have been previously analyzed. Through the monitoring of the soil hydrological conditions, a detailed description of the physical-mechanical triggering mechanism of landslides and of the hydrological conditions leading to failure, in relation to the site-specific characteristics of the involved soils and stratigraphy, has been obtained. In particular, field measurements in time of some unsaturated soil hydrological parameters, such as soil water content and pore water pressure, proved of paramount importance. In the study area, the triggering mechanism of rainfall-induced shallow landslides is linked to the uprising of a perched water table present in wet months (winter and spring months) in the slope soils in correspondence of particularly intense rainfalls.

Field measurements also allowed to calibrate in a reasonable way a physically-based susceptibility model, which takes into account unsaturated soil conditions, such as the TRIGRS-Unsaturated model.

NHESSD
2, 7409–7464, 2014

By applying the typical soil hydrological conditions, in terms of perched-water table in wetting periods in agreement with field observations, the pore water pressure evaluated by the TRIGRS-Unsaturated model essentially agree with the measurements acquired at the monitored test-site slope for different selected rainfall events.

The correct evaluation of the time trend of pore water pressure during a rainfall event is fundamental for assessing the shallow landslides susceptibility of an area in which the slope soils have conditions of not complete saturation. On the basis of the good comparison between measured and modelled pore water pressure for the monitored rainfall events, it was possible considering as reliable also the pore water pressure modelled in correspondence of the 27–28 April 2009 event, particularly in terms of correct discrimination of the increase in pore water pressure due to the intensity peaks during the rainfall.

The calibration phase carried out at the test-site slope shows the correct assessment of the shallow landslides scarps of April 2009 event. After this phase, the same model has been applied at regional scale on the surrounding area (13.4 km^2 wide), which had been greatly affected by many shallow landslides in the same event of 27–28 April 2009. Once the reliability of hydro-mechanical modelling through TRIGRS-Unsaturated model was verified with the improvement linked to the monitored soil hydrological behaviours, it was possible to evaluate the role played by the type of unit mapping on the assessment of unstable areas. Different unit mapping (geological and pedological) have been considered, which divided the study area in different classes, characterized by a different set of both hydrological and geotechnical soil properties.

The results obtained at regional scale, by comparing real and predicted unstable areas, are quite satisfactory in terms of both success and error indexes.

The main differences on the models were linked to SI values of the Fs maps, while the EI values kept steady around 10 % taking into account different mapping (Fig. 13). The best result is obtained by considering a pedological zoning of the study area, which leads to an increase of SI of about 5 % higher than that obtained by using a geological mapping (respectively 78.9 and 73.3 %; Fig. 13).

NHESSD
2, 7409–7464, 2014

Moreover, the results obtained by TRIGRS-Unsaturated model based on the geological units were compared with the results obtained through other physically-based models in the same area (Zizioli et al., 2013). The research demonstrates how implementing reliable hydrological conditions, derived from the analysis of the typical soil hydrological behaviour and from continuous field monitoring, allows an improvement in the prediction of shallow landslides source areas. In fact, based on the same zoning (geological units) of the soil in the study area, TRIGRS-Unsaturated model has a quite higher degree of success in respect to the models (TRIGRS-Saturated, SINMAP, SLIP) applied in the past for the same area, which considered different hydrological modelling and different hydrological input data (Zizioli et al., 2013). The improvement is testified by a significant reduction, on the order of the 20 %, of the EI, which is linked to a lower overestimation of the computed unstable areas. Furthermore, the SI value of TRIGRS-Unsaturated model is higher than the other models, thus testifying a better assessment of the shallow landslides susceptibility.

The TRIGRS-Unsaturated model results are different, although very close to those previously obtained through TRIGRS-saturated model (Zizioli et al., 2013). This difference was already shown in other case studies (Sorbino et al., 2007, 2010), even if neglecting the effects played by the not completely saturated conditions of the soils can be quite costly on the assessment of shallow landslides susceptibility (Sorbino et al., 2010).

The obtained results confirm the necessity of verifying the reliability of a physically-based model before its implementation for the shallow landslides susceptibility assessment. The scheme followed in this work can be applied also in other similar contexts for the identification of slopes prone to shallow landslides and for a better land use planning. In particular, future developments will be the application of TRIGRS-Unsaturated model in areas affected by shallow landslides and characterized by the extensive presence of slopes cultivated with vineyards as in Oltrepò Pavese. Furthermore, the role played by wine plant roots on soil reinforcement will be considered, allowing for the development of agricultural best management practices to prevent instability phenomena.

NHESSD
2, 7409–7464, 2014

Acknowledgements. We thank M. A. Leoni of the Riccagioia S.C.P.A. – Centro di Ricerca Formazione e Servizi della Vite e del Vino for the pedological analyses of the soil of the monitored slope. We also thank M. Setti of the Department of Earth and Environmental Sciences of University of Pavia for the X-Ray diffraction analyses of the soil of the monitored slope.

References

Alpert, P., Bengai, T., Baharad, A., Benjamini, Y., Yekutieli, D., Colacino, M., Diodato, L., Ramis, C., Homar, V., Romero, R., Michaelides, S., and Manes, A.: The paradoxical increase of Mediterranean extreme daily rainfall in spite of decrease in total values, Geophys. Res. Lett., 29, 31-1–31-4, doi:10.1029/2001GL013554, 2002.

Baum, R. L., Savage, W. Z., and Godt, J. W.: TRIGRS – a FORTRAN Program for Transient Rainfall Infiltration and Grid-Based Regional Slope-Stability Analysis, Open-File Report 02-0424, US Geological Survey, Denver, 35 pp., 2002.

Baum, R. L., Savage, W. Z., and Godt, J. W.: TRIGRS – a FORTRAN Program for Transient Rainfall Infiltration and Grid-Based Regional Slope-Stability Analysis, version 2.0, Open-File Report 2008-1159, US Geological Survey, Denver, 81 pp., 2008.

Baum, R. L., Godt, J. W., and Savage, W. Z.: Estimating the timing and location of shallow rainfallinduced landslides using a model for transient, unsaturated infiltration, J. Geophys. Res., 115, F03013, doi:10.1029/2009JF001321, 2010.

Baum, R. L., Godt, J. W., and Coe, J. A.: Assessing susceptibility and timing of shallow landslide and debris flow initiation in the Oregon Coast Range, USA, in: Proceedings of the 5th International Conference on Debris Flow Hazards Mitigation, Mechanics, Prediction and Assessment, 14–17 June 2011, edited by: Genevois, R., Hamilton, D. L., and Prestininzi, A., Padua, Italy, 825–834, 2011.

Bittelli, M., Valentino, R., Salvatorelli, F., and Rossi Pisa, P.: Monitoring soil-water and displacement conditions leading to landslide occurrence in partially saturated clays, Geomorphology, 173–174, 161–173, 2011

Bordoni, M., Meisina, C., Zizioli, D., Valentino, R., Bittelli, M., and Chersich, S.: Rainfall-induced landslides: slope stability analysis through field monitoring, in: Landslide Science for a Safer Geoenvironment, vol. 3, edited by: Sassa, K., Canuti, P., and Yin, Y., Springer International Publishing, Heidelberg, 273–279, 2014.

NHESSD

2, 7409–7464, 2014

Braga, G., Braschi, G., Calculli, S., Caucia, F., Cerro, A., Colleselli, F., Grisolia, M., Piccio, A., Rossetti, R., Setti, M., Soggetti, F., and Veniale, F.: I fenomeni franosi nell'Oltrepo Pavese: tipologia e cause, Geologia Applicata e Idrogeologia, 20, 621–666, 1985.

Campus, S., Forlati, F., Susella, G., and Tamberlani, F.: Frane per mobilizzazione delle coperture detritiche, in: Eventi Alluvionali in Piemonte, Regione Piemonte, Turin, 266–287, 1998.

Comegna, L.: Regional analysis of rainfall-induced landslides. The case of Camaldoli hill, Naples: test case nr. 1 – October 2004; test case nr. 2 – September 2005, Centro euro-Mediterraneo per i Cambiamenti Climatici CMCC, Lecce, 32 pp., 2008.

Conrad, O.: SAGA – program structure and current state of implementation, in: SAGA – Analysis and Modelling Applications, edited by: Böhner, J., McCloy, K. R., and Strobl, J., Göttinger Geographische Abhandlungen, Göttingen, 39–52, 2006.

Crosta, G. B. and Frattini, P.: Distributed modelling of shallow landslides triggered by intense rainfall, Nat. Hazards Earth Syst. Sci., 3, 81–93, doi:10.5194/nhess-3-81-2003, 2003.

Cruden, D. M. and Varnes, D. J.: Landslide types and processes, in: Landslides: Investigation and Mitigation, edited by: Turner, A. K. and Schuster, R. L., National Academy Press, Washington, D.C., 36–75, 1996.

D'Amato Avanzi, G., Giannecchini, R., and Puccinelli, A.: The influence of the geological and geomorphological settings on shallow landslides. An example in a temperate climate environment: the 19 June 1996 event in northwestern Tuscany (Italy), Eng. Geol., 73, 215–228, 2003.

Damiano, E., Olivares, L., and Picarelli, L.: Steep-slope monitoring in unsaturated pyroclastic soils, Eng. Geol., 137–138, 1–12, 2012.

Dapporto, S., Aleotti, P., Casagli, N., and Polloni, G.: Analysis of shallow failures triggered by the 14–16 November 2002 event in the Albaredo valley, Valtellina (Northern Italy), Adv. Geosci., 2, 305–308, doi:10.5194/adgeo-2-305-2005, 2005.

ERSAL: I suoli dell'Oltrepo Pavese, Milan, 2001.

Galve, J. P., Cevasco, A., Brandolini, P., and Soldati, M.: Assessment of shallow landslide risk mitigation measures based on land use planning through probabilistic modelling, Landslides, doi:10.1007/s10346-014-0478-9, in press, 2014.

Gardner, W. R.: Some steady-state solutions of the unsaturated moisture flow equation with application to evaporation from a water table, Soil Sci., 85, 228–232, 1958.

NHESSD

2, 7409–7464, 2014

From slope- to regional-scale shallow landslides susceptibility assessment

M. Bordoni et al.

Ghezzehei, T. A., Kneafsey, T. J., and Su, G. W.: Correspondence of the Gardner and van Genuchten/Mualem relative permeability function parameters, Water Resour. Res., 43, W10417, doi:10.1029/2006WR005339, 2007.

Godt, J. W., Baum, R. L., Savage, W. Z., Salciarini, D., Schulz, W. H., and Harp, E. L.: Transient deterministic shallow landslide modelling: requirements for susceptibility and hazard assessment in a GIS framework, Eng. Geol., 102, 214–226, 2008a.

Godt, J. W., Schulz, W. H., Baum, R. L., and Savage, W. Z.: Modelling rainfall conditions for shallow landsliding in Seattle, Washington, in: Landslides and Engineering Geology of the Seattle, Washington, Area, edited by: Baum, R. L., Godt, J. W., and Highland, L. M., The Geological Society of America, Boulder, 137–152, 2008b.

Grelle, G., Soriano, M., Revellino, P., Guerriero, L., Anderson, M. G., Diambra, A., Fiorillo, F., Esposito, L., Diodato, N., and Guadagno, F. M.: Space–time prediction of rainfall-induced shallow landslides through a combined probabilistic/deterministic approach, optimized for initial water table conditions, B. Eng. Geol. Environ., 73, 877–890, doi:10.1007/s10064-013-0546-8, 2014.

Howard, T. R., Baldwin, J. E., and Donley, H. E.: Landslides in Pacifica California, caused by the storm, in: Landslides, Floods and Marine Effects of the Storm of 3–5 January 1982 in the San Francisco Bay Region, California: US Geological Survey Professional Paper 1434, edited by: Ellen, S. D. and Wieckzoreck, G. F., US Geological Survey, Denver, 163–184, 1988.

IUSS Working Group WRB: World Reference for Soil Resources 2006, first update 2007, World Soil Resources Reports 103, FAO, Rome, 2007.

Iverson, R. M.: Landslide triggering by rain infiltration, Water Resour. Res., 36, 1897–1910, 2000.

Lanni, C., Borga, M., Rigon, R., and Tarolli, P.: Modelling shallow landslide susceptibility by means of a subsurface flow path connectivity index and estimates of soil depth spatial distribution, Hydrol. Earth Syst. Sci., 16, 3959–3971, doi:10.5194/hess-16-3959-2012, 2012.

Liao, Z., Hong, Y., Kirschbaum, D., Adler, R. F., Gourley, J. J., and Wooten, R.: Evaluation of TRIGRS (transient rainfall infiltration and grid-based regional slope-stability analysis)'s predictive skill for hurricane-triggered landslides: a case study in Macon County, North Carolina, Nat. Hazards, 58, 325–339, doi:10.1007/s11069-010-9670-y, 2011.

Lim, T. T., Rahardjo, H., Chang, M. F., and Fredlund, D. G.: Effect of rainfall on matric suctions in a residual soil slope, Can. Geotech. J., 33, 618–628, 1996.

NHESSD
2, 7409–7464, 2014

Lu, N. and Godt, J. W.: Infinite-slope stability under steady unsaturated seepage conditions, Water Resour. Res., 44, W11404, doi:10.1029/2008WR006976, 2008.
Marquardt, D. W.: An algorithm for least-squares estimation of non-linear parameters, J. Soc. Ind. App. Math., 11, 431–441, 1963.
Meisina, C.: Characterisation of weathered clayey soils responsible for shallow landslides, Nat. Hazards Earth Syst. Sci., 6, 825–838, doi:10.5194/nhess-6-825-2006, 2006.
Meisina, C. and Scarabelli, S.: A comparative analysis of terrain stability models for predicting shallow landslides in colluvial soils, Geomorphology, 87, 207–223, 2007.
Montgomery, D. R. and Dietrich, W. E.: A physically based model for the topographic control on shallow landsliding, Water Resour. Res., 30, 1153–1171, 1994.
Montrasio, L. and Valentino, R.: A model for triggering mechanisms of shallow landslides, Nat. Hazards Earth Syst. Sci., 8, 1149–1159, doi:10.5194/nhess-8-1149-2008, 2008.
Mualem, Y.: A new model predicting the hydraulic conductivity of unsaturated porous media, Water Resour. Res., 12, 513–522, 1976.
Pack, R. T., Tarboton, D. G., and Goodwin, C. G.: SINMAP 2.0 – a Stability Index Approach to Terrain Stability Hazard Mapping, User's Manual, produced in ArcView Avenue and C++ for Forest Renewal B. C. under Research Contract No. PA97537-0RE, available at: http://www.neng.usu.edu/cee/faculty/dtarb/sinmap.pdf (last access: 10 December 2014), 1999.
Papa, M. N., Medina, V., Ciervo, F., and Bateman, A.: Derivation of critical rainfall thresholds for shallow landslides as a tool for debris flow early warning systems, Hydrol. Earth Syst. Sci., 17, 4095–4107, doi:10.5194/hess-17-4095-2013, 2013.
Park, D. W., Nikhil, N. V., and Lee, S. R.: Landslide and debris flow susceptibility zonation using TRIGRS for the 2011 Seoul landslide event, Nat. Hazards Earth Syst. Sci., 13, 2833–2849, doi:10.5194/nhess-13-2833-2013, 2013.
Peters, A. and Durner, W.: Simplified evaporation method for determining soil hydraulic properties, J. Hydrol., 356, 147–162, 2008.
Qiu, C., Esaki, T., Xie, M., Mitani, Y., and Wang, C.: Spatiotemporal estimation of shallow landslide hazard triggered by rainfall using a three-dimensional model, Environ. Geol., 52, 1569–1579, 2007.
Rawlins, S. L. and Campbell, G. S.: Water potential: thermocouple psychrometry, in: Methods of Soil Analysis Part 1, 2nd Edn., Agron. Monogr. 9, Soil Science Society of America, Madison, WI, 597–618, 1986.

NHESSD
2, 7409–7464, 2014

Rossetti, R. and Ottone, C.: Esame preliminare delle condizioni pluviometriche dell'Oltrepo Pavese e dei valori critici delle precipitazioni in relazione ai fenomeni di dissesto franoso, Geologia Applicata e Idrogeologia, 24, 83–99, 1979.

Rossi, G., Catani, F., Leoni, L., Segoni, S., and Tofani, V.: HIRESSS: a physically based slope stability simulator for HPC applications, Nat. Hazards Earth Syst. Sci., 13, 151–166, doi:10.5194/nhess-13-151-2013, 2013.

Salciarini, D., Godt, J. W., Savage, W. Z., Conversini, R., Baum, R. L., and Michael, J. A.: Modelling regional initiation of rainfall-induced shallow landslides in the eastern Umbria Region of central Italy, Landslides, 3, 181–194, 2006.

Salciarini, D., Godt, J. W., Savage, W. Z., Baum, R. L., and Conversini, R.: Modelling landslide recurrence in Seattle, Washington, USA, Eng. Geol., 102, 227–237, 2008.

Schaap, M. G., Feike, L. J., and Van Genuchten, M. T.: ROSETTA: a computer program for estimating soil hydraulic parameters with hierarchical pedotransfers functions, J. Hydrol., 251, 163–176, 2001.

Schindler, U.: Ein Schnellverfahren zur Messung der Wasserleitfähigkeit im teilgesättigten Boden an Stechzylinderproben, Arch. Acker. Pfl. Boden., 24, 1–7, 1980.

Schnellmann, R., Busslinger, M., Schneider, H. R., and Rahardjo, H.: Effect of rising water table in an unsaturated slope, Eng. Geol., 114, 71–83, 2010.

Simoni, A., Berti, M., Generali, M., Elmi, C., and Ghirotti, M.: Preliminary result from pore pressure monitoring on an unstable clay slope, Eng. Geol., 73, 117–128, 2004.

Smethurst, J. A., Clarke, D., and Powrie, D.: Factors controlling the seasonal variation in soil water content and pore water pressures within a lightly vegetated clay slope, Geotechnique, 62, 429–446, 2012.

Sorbino, G., Sica, C., Cascini, L., and Cuomo, S.: On the forecasting of flowslides triggering areas using physically based models, in: Proceedings of 1st North American Landslides Conference, vol. 1, AEG Special Publication 23, Vail, 305–315, 2007.

Sorbino, G., Sica, C., and Cascini, L.: Susceptibility analysis of shallow landslides source areas using physically based models, Nat. Hazards, 53, 313–332, 2010.

Springman, S. M., Thielen, A., Kienzler, P., and Friedel, S.: A long-term field study for the investigation of rainfall-induced landslides, Geotechnique, 14, 1177–1193, 2013.

Srivastava, R. and Yeh, T.-C. J.: Analytical solutions for one-dimensional, transient infiltration toward the water table in homogeneous and layered soils, Water Resour. Res., 27, 753–762, 1991.

NHESSD

2, 7409–7464, 2014

Tiranti, D. and Rabuffetti, D.: Estimation of rainfall thresholds triggering shallow landslides for an operational warning system implementation, Landslides, 7, 471–481, 2010.
Vanapalli, S. K., Fredlund, D. G., Pufahl, D. E., and Clifton, A. W.: Model for the prediction of shear strength with respect to soil suction, Can. Geotech. J., 33, 379–392, 1996.
Van Genuchten, M. T.: A closed-form equation for predicting the hydraulic conductivity of unsaturated soils, Soil Sci. Soc. Am. J., 44, 892–898, 1980.
Vercesi, P. and Scagni, G.: Osservazioni sui depositi conglomeratici dello sperone collinare di Stradella, Rendiconti della Società Geologica Italiana, 7, 23–26, 1984.
Wu, W. and Sidle, R. C.: A distributed slope stability model for steep forested hillslopes, Water Resour. Res., 31, 2097–2110, 1995.
Zhan, T. L. T., Ng, C. W. W., and Fredlund, D. G.: Instrumentation of an unsaturated expansive soil slope, Geotech. Test J., 30, 1–11, 2006.
Zizioli, D., Meisina, C., Valentino, R., and Montrasio, L.: Comparison between different approaches to modeling shallow landslide susceptibility: a case history in Oltrepo Pavese, Northern Italy, Nat. Hazards Earth Syst. Sci., 13, 559–573, doi:10.5194/nhess-13-559-2013, 2013.
Zizioli, D., Meisina, C., Bordoni, M., and Zucca, F.: Rainfall-triggered shallow landslides mapping through Pleiades images, in: Landslide Science for a Safer Geoenvironment, vol. 2, edited by: Sassa, K., Canuti, P., and Yin, Y., Springer International Publishing, Heidelberg, 325–329, 2014.

NHESSD
2, 7409–7464, 2014

Table 1. Selected geotechnical and mechanical features of the monitored slope soil and weathered bedrock: grain size distribution (Gravel, Sand, Silt, Clay), liquid limit (w_L), plasticity index (P_I), unit weight (γ), friction angle (φ'), cohesion (c').

Representative depth	Gravel	Sand	Silt	Clay	w_L	P_I	γ	φ	c'
m	(%)	(%)	(%)	(%)	(%)	(%)	(kN m^{-3})	(°)	(kPa)
0.2	12.3	12.5	53.9	21.3	39.8	17.2	17.0		
0.4	1.5	11.4	59.4	27.7	38.5	14.3	16.7	31	0.0
0.6	8.5	13.2	51.1	27.2	40.3	15.7	16.7	31	0.0
1.0	2.4	12.2	56.4	29.0	39.2	15.9	18.6	33	0.0
1.2	0.5	7.5	65.6	26.4	41.9	16.5	18.3	26	29.0
1.4	0.2	75.0	24.8	0.0	–	–	18.1		

NHESSD
2, 7409–7464, 2014

Table 2. Hydrological properties of the monitored slope soil and weathered bedrock.

Representative depth m	α (kPa^{-1})	n (-)	θ_s ($m^3\,m^{-3}$)	θ_r ($m^3\,m^{-3}$)	K_s ($m\,s^{-1}$)
0.2	0.013	1.43	0.43	0.03	2.5×10^{-6}
0.4	–	–	–	–	–
0.6	0.010	1.40	0.42	0.01	1.5×10^{-6}
1.0	0.009	1.38	0.39	0.02	1.0×10^{-6}
1.2	0.007	1.34	0.40	0.01	0.5×10^{-6}
1.4	–	–	–	–	–

NHESSD
2, 7409–7464, 2014

Table 3. Mean geotechnical and mechanical characteristics of the mapping units of the study area.

	w_L (%)	P_I (%)	Gravel (%)	Sand (%)	Silt (%)	Clay (%)	γ (kN m^{-3})	φ' (°)	c' (kPa)
Geological unit									
Monte Arzolo Sandstones	43.9	22.7	2.4	16.0	55.6	26.0	17.9	26	1.9
Rocca Ticozzi Conglomerates	41.2	18.5	5.1	17.9	53.1	23.9	17.7	27	1.5
Sant'Agata Fossili Marls	42.0	22.6	1.7	8.3	52.9	37.1	18.0	26	2.0
Gessoso-Solfifera Formation	41.9	21.2	2.0	9.1	53.4	29.5	17.8	24	1.8
Pedological unit									
BRS1	42.3	21.3	1.3	10.5	58.2	30.0	17.0	24	1.2
FGE1	52.4	31.8	1.5	8.3	46.9	43.3	17.5	26	2.0
ILM1/RUM1	40.7	18.1	4.8	19.3	52.4	23.5	18.1	26	1.5
MRL1	42.2	21.0	3.3	12.1	56.7	27.9	18.1	25	1.5

NHESSD
2, 7409–7464, 2014

Table 4. Mean hydrological properties of the mapping units of the study area.

	θ_s ($m^3\,m^{-3}$)	θ_r ($m^3\,m^{-3}$)	α (kPa^{-1})	n (–)	K_s ($m\,s^{-1}$)
Geological unit					
Monte Arzolo Sandstones	0.44	0.06	0.006	1.57	1.5×10^{-6}
Rocca Ticozzi Conglomerates	0.43	0.05	0.006	1.58	1.5×10^{-6}
Sant'Agata Fossili Marls	0.46	0.08	0.007	1.54	1.4×10^{-6}
Gessoso-Solfifera Formation	0.48	0.08	0.010	1.46	1.4×10^{-6}
Pedological unit					
BRS1	0.46	0.07	0.007	1.53	1.5×10^{-6}
FGE1	0.49	0.09	0.012	1.39	1.5×10^{-6}
ILM1/RUM1	0.43	0.05	0.006	1.58	1.4×10^{-6}
MRL1	0.45	0.08	0.007	1.55	1.4×10^{-6}

NHESSD
2, 7409–7464, 2014

Table 5. Soil parameters used as input data for TRIGRS.

	γ (kN m^{-3})	φ' (°)	c' (kPa)	θ_s (m^3 m^{-3})	θ_r (m^3 m^{-3})	α_G (kPa^{-1})	K_s (m s^{-1})	D_0 (m s^{-1})
Geological unit								
Monte Arzolo Sandstones	17.9	26	1.9	0.44	0.06	0.012	1.5×10^{-6}	3.0×10^{-6}
Rocca Ticozzi Conglomerates	17.7	27	1.5	0.43	0.05	0.012	1.5×10^{-6}	3.0×10^{-6}
Sant'Agata Fossili Marls	18.0	26	2.0	0.46	0.08	0.014	1.4×10^{-6}	2.8×10^{-6}
Gessoso-Solfifera Formation	17.8	24	1.8	0.48	0.08	0.019	1.4×10^{-6}	2.8×10^{-6}
Pedological unit								
BRS1	17.0	24	1.2	0.46	0.07	0.014	1.5×10^{-6}	3.0×10^{-6}
FGE1	17.5	26	2.0	0.49	0.09	0.022	1.5×10^{-6}	3.0×10^{-6}
ILM1/RUM1	18.1	26	1.5	0.43	0.05	0.012	1.4×10^{-6}	2.8×10^{-6}
MRL1	18.1	25	1.5	0.45	0.08	0.012	1.4×10^{-6}	2.8×10^{-6}

NHESSD
2, 7409–7464, 2014

Table 6. Selected rainfall events for the implementation of TRIGRS-Unsaturated features.

Rainfall event (date time)	Duration (h)	Cumulated rain (mm)	Mean intensity ($mm\,h^{-1}$)	Minimum intensity ($mm\,h^{-1}$)	Maximum intensity ($mm\,h^{-1}$)
26 Apr 2009 06:00 LT 28 Apr 2009 08:00 LT	62	159.4	2.6	0.0	22.6
23 Mar 2013 17:00 LT 25 Mar 2013 20:00 LT	40	31.5	0.8	0.1	2.9
30 Mar 2013 07:00 LT 30 Mar 2013 19:00 LT	13	24.5	1.9	0.1	3.8
4 Apr 2013 16:00 LT 5 Apr 2013 17:00 LT	26	29.5	1.1	0.1	2.8
20 Apr 2013 11:00 LT 22 Apr 2013 16:00 LT	54	47.7	0.9	0.0	8.2
18 Jan 2014 07:00 LT 20 Jan 2014 02:00 LT	44	34.6	0.8	0.0	3.9
28 Feb 2014 18:00 LT 2 Mar 2014 12:00 LT	43	68.9	1.6	0.0	4.4

NHESSD
2, 7409–7464, 2014

Table 7. Measured initial-final pore water pressure values vs. computed by TRIGRS-Unsaturated ones for the selected rainfall events at 0.6 m from ground in correspondence of the monitoring station in the study area.

Rainfall event (date time)	Initial pore water pressure at −0.6 m (kPa)		Final pore water pressure at −0.6 m (kPa)		RMSE (kPa)
	Meas.	TRIGRS	Meas.	TRIGRS	
23 Mar 2013 17:00 LT 25 Mar 2013 20:00 LT	−6.1	−5.1	−4.6	−3.6	1.1
30 Mar 2013 07:00 LT 30 Mar 2013 19:00 LT	−5.9	−5.0	−3.8	−3.7	0.9
4 Apr 2013 16:00 LT 5 Apr 2013 17:00 LT	−6.3	−5.0	−4.3	−3.5	1.5
20 Apr 2013 11:00 LT 22 Apr 2013 16:00 LT	−8.1	−9.0	−4.5	−6.3	1.3
18 Jan 2014 07:00 LT 20 Jan 2014 02:00 LT	−5.5	−4.5	−4.4	−2.8	1.2
28 Feb 2014 18:00 LT 2 Mar 2014 12:00 LT	−6.1	−5.6	−4.9	−2.2	1.4

NHESSD
2, 7409–7464, 2014

Table 8. Measured initial-final pore water pressure values vs. computed by TRIGRS-Unsaturated ones for the selected rainfall events at 1.2 m from ground in correspondence of the monitoring station in the study area.

Rainfall event (date time)	Initial pore water pressure at −1.2 m (kPa)		Final pore water pressure at −1.2 m (kPa)		RMSE (kPa)
	Meas.	TRIGRS	Meas.	TRIGRS	
23 Mar 2013 17:00 LT 25 Mar 2013 20:00 LT	−0.4	−0.1	0.5	1.2	0.8
30 Mar 2013 07:00 LT 30 Mar 2013 19:00 LT	−0.5	−0.6	0.6	0.1	0.2
4 Apr 2013 16:00 LT 5 Apr 2013 17:00 LT	−0.5	−1.0	−0.9	0.4	0.4
20 Apr 2013 11:00 LT 22 Apr 2013 16:00 LT	−1.6	−0.7	0.7	−0.4	0.8
18 Jan 2014 07:00 LT 20 Jan 2014 02:00 LT	−1.2	−0.9	−0.2	−0.8	0.6
28 Feb 2014 18:00 LT 2 Mar 2014 12:00 LT	−0.7	−0.6	0.5	2.5	1.2

NHESSD
2, 7409–7464, 2014

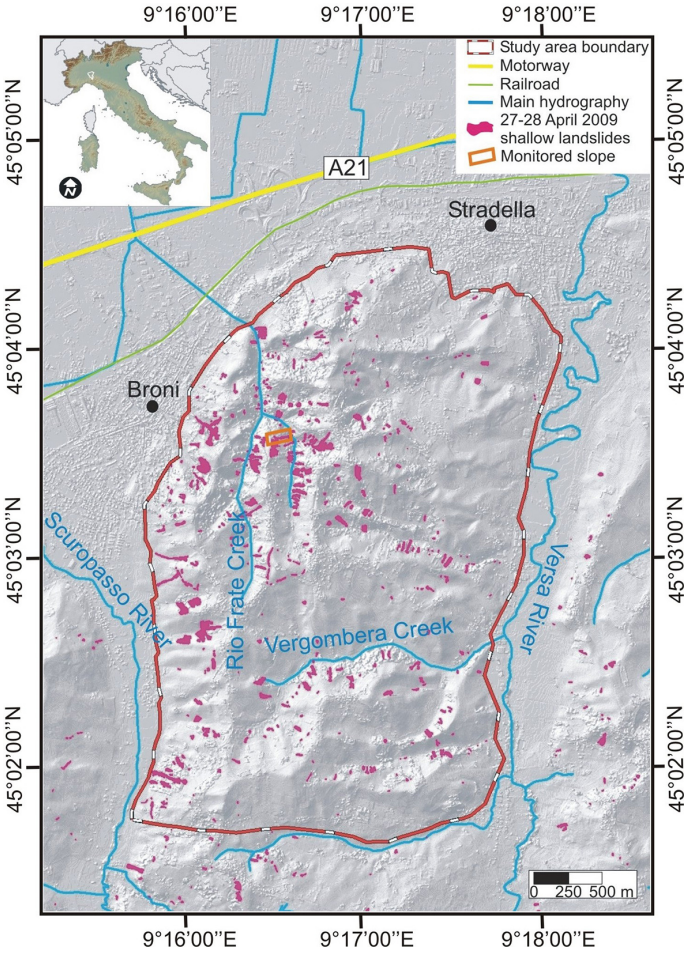

Figure 1. Location of the study area.

NHESSD
2, 7409–7464, 2014

From slope- to regional-scale shallow landslides susceptibility assessment

M. Bordoni et al.

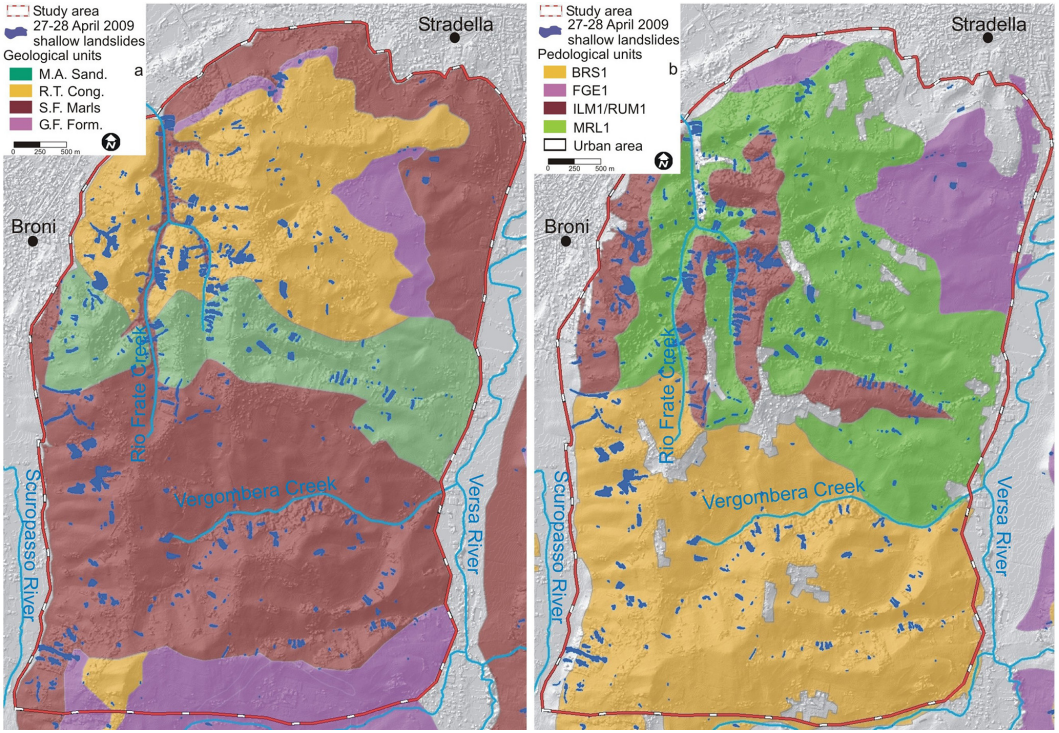

Figure 2. Geological **(a)** and pedological **(b)** units distribution across the study area.

NHESSD
2, 7409–7464, 2014

From slope- to regional-scale shallow landslides susceptibility assessment

M. Bordoni et al.

Figure 3. Examples of rainfall-induced shallow landslides occurred in the study area during the event of 27–28 April 2009, according to Cruden and Varnes' (1996) and Campus et al.'s (1998) classifications: **(a)** incipient translational slides; **(b)** translational soil slides; **(c)** complex landslides; **(d)** disintegrating soil slips.

NHESSD
2, 7409–7464, 2014

From slope- to regional-scale shallow landslides susceptibility assessment

M. Bordoni et al.

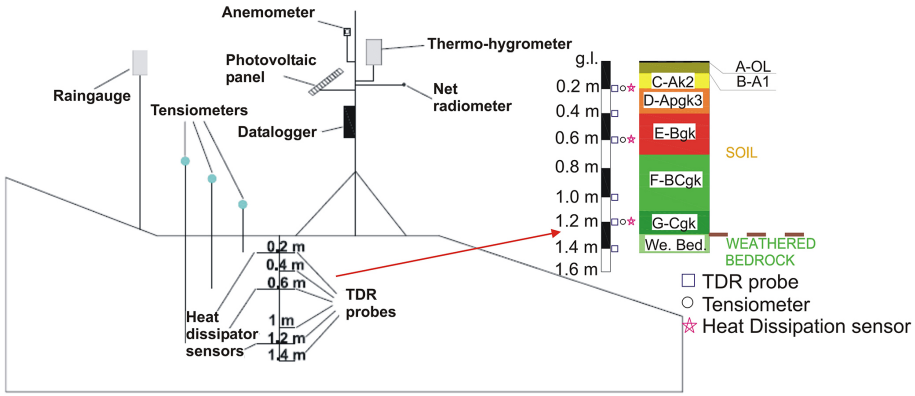

Figure 4. Schematic representation of the monitoring station installed in the study area.

NHESSD
2, 7409–7464, 2014

From slope- to regional-scale shallow landslides susceptibility assessment

M. Bordoni et al.

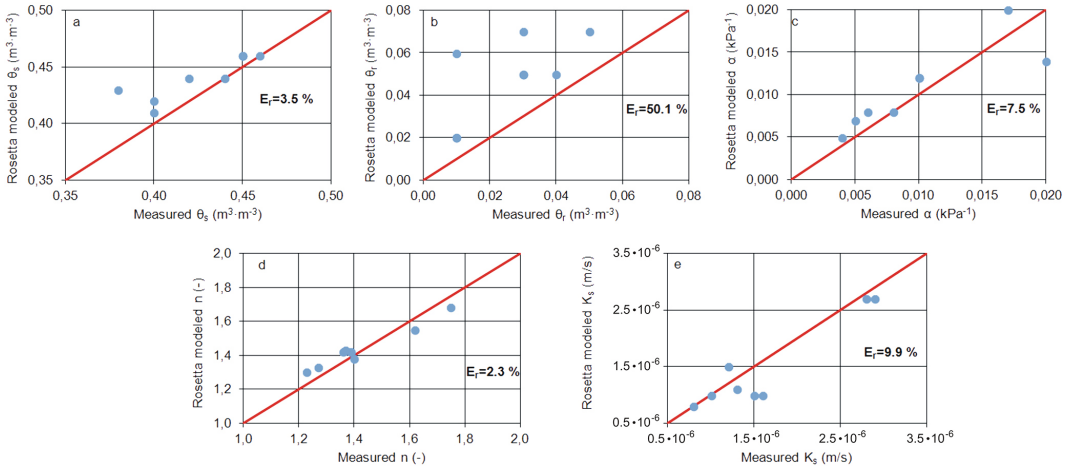

Figure 5. Comparison between measured and modelled parameters of Mualem and Van Genuchten models for some soil samples taken in the study area, obtained through Rosetta pedotransfer function: **(a)** θ_s; **(b)** θ_r; **(c)** α; **(d)** n; **(e)** K_s.

NHESSD
2, 7409–7464, 2014

From slope- to regional-scale shallow landslides susceptibility assessment

M. Bordoni et al.

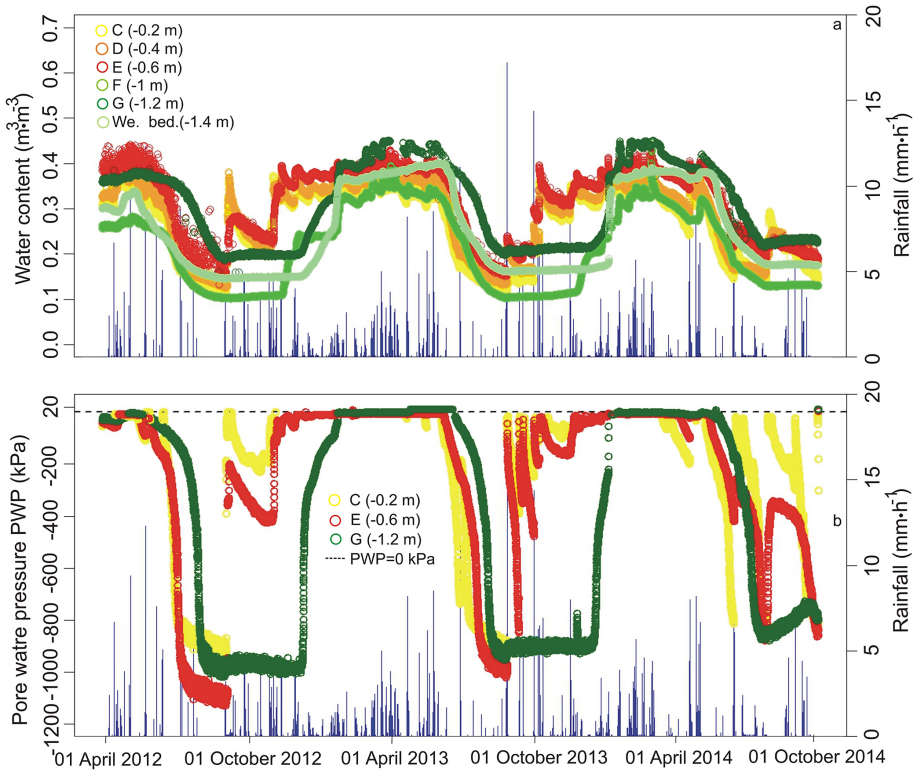

Figure 6. Monitored soil and weathered bedrock water content **(a)** and pore water pressure dynamics **(b)** at the monitored test-site slope in the study area.

NHESSD
2, 7409–7464, 2014

From slope- to regional-scale shallow landslides susceptibility assessment

M. Bordoni et al.

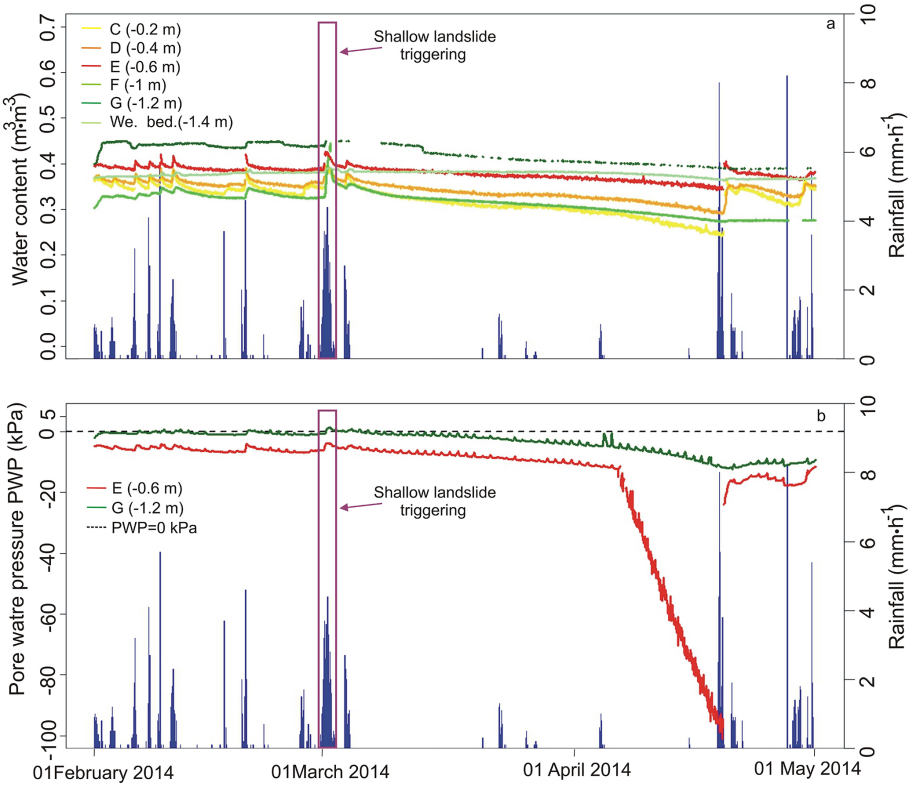

Figure 7. Monitored soil and weathered bedrock water content **(a)** and pore water pressure dynamics **(b)** at the monitored test-site slope between 1 February–1 May 2014.

NHESSD
2, 7409–7464, 2014

From slope- to regional-scale shallow landslides susceptibility assessment

M. Bordoni et al.

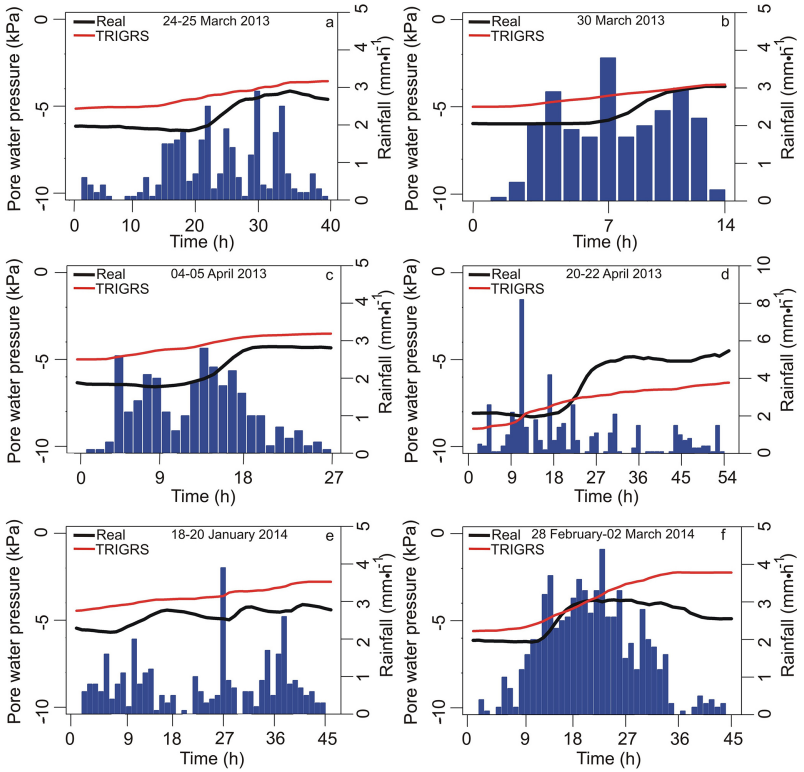

Figure 8. Comparison between measured and estimated by TRIGRS-Unsaturated pore water pressure trends at 0.6 m from ground in correspondence of the monitoring station for selected rainfall events: **(a)** 23–25 March 2013; **(b)** 30 March 2013; **(c)** 4–5 April 2013; **(d)** 20–22 April 2013; **(e)** 18–20 January 2014; **(f)** 28 February–2 March 2014.

NHESSD
2, 7409–7464, 2014

From slope- to regional-scale shallow landslides susceptibility assessment

M. Bordoni et al.

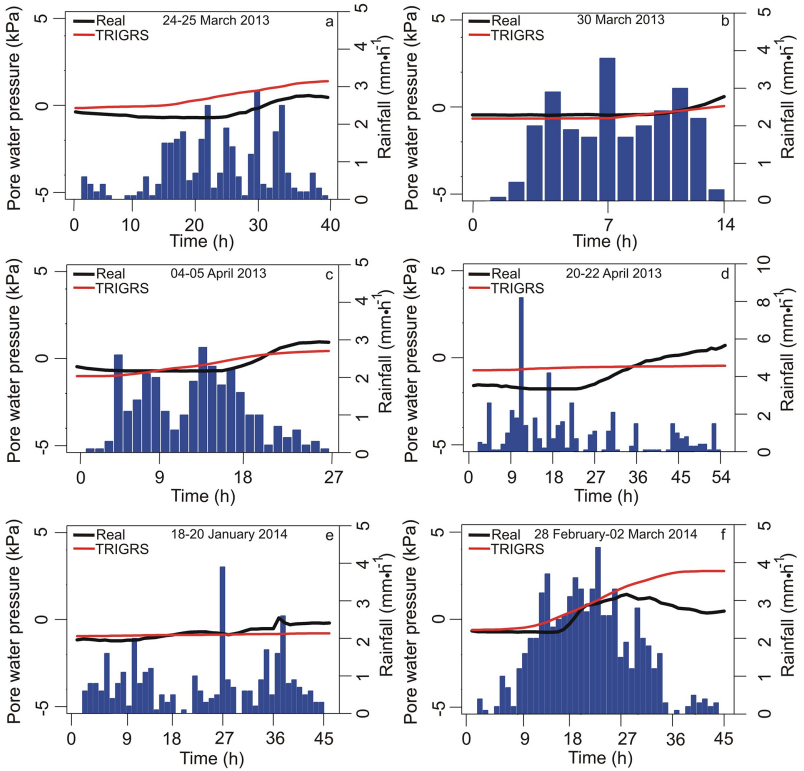

Figure 9. Comparison between measured and estimated by TRIGRS-Unsaturated pore water pressure trends at 1.2 m from ground in correspondence of the monitoring station for selected rainfall events: **(a)** 23–25 March 2013; **(b)** 30 March 2013; **(c)** 4–5 April 2013; **(d)** 20–22 April 2013; **(e)** 18–20 January 2014; **(f)** 28 February–2 March 2014.

NHESSD
2, 7409–7464, 2014

From slope- to regional-scale shallow landslides susceptibility assessment

M. Bordoni et al.

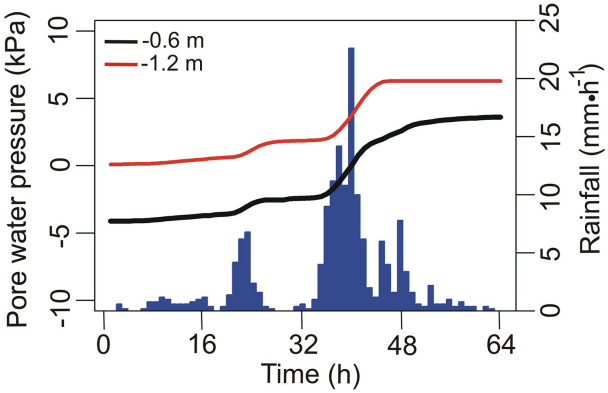

Figure 10. Modelled by TRIGRS-Unsaturated pore water pressure for 27–28 April 2009 event in correspondence of the monitoring station in the study area.

NHESSD
2, 7409–7464, 2014

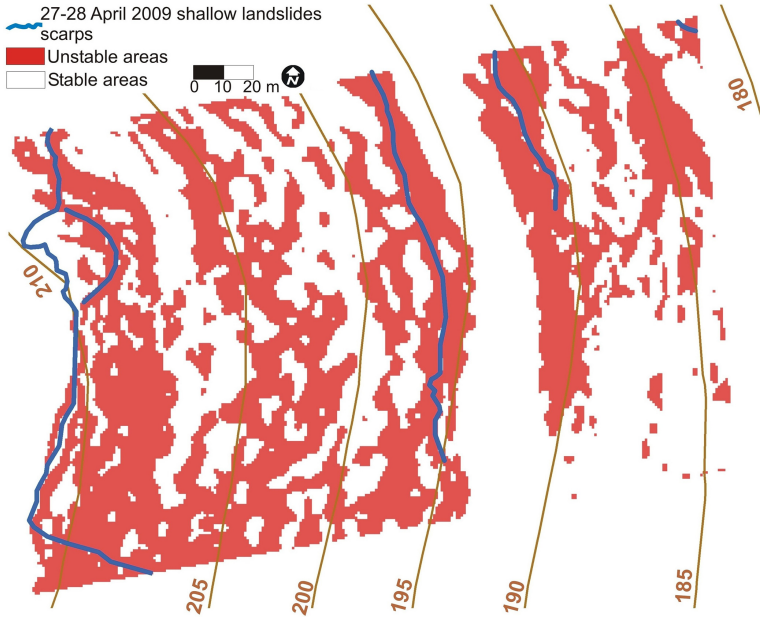

Figure 11. Shallow landslides susceptibility scenarios corresponding to the 27–28 April 2009 event for the monitored test-site slope by implementing TRIGRS-Unsaturated model for a DEM with grid size of 2 m × 2 m.

NHESSD
2, 7409–7464, 2014

From slope- to regional-scale shallow landslides susceptibility assessment

M. Bordoni et al.

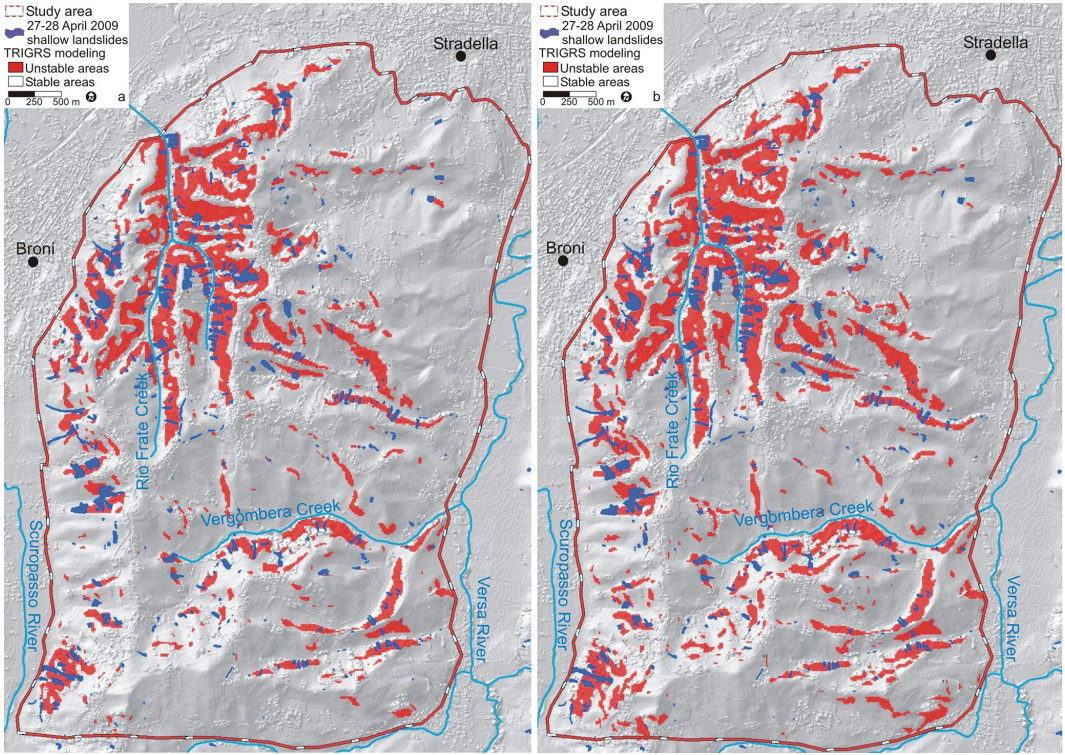

Figure 12. Shallow landslides susceptibility scenarios corresponding to the 27–28 April 2009 event for the study area by using TRIGRS-Unsaturated model: **(a)** geological mapping units; **(b)** pedological mapping units.

NHESSD
2, 7409–7464, 2014

From slope- to regional-scale shallow landslides susceptibility assessment

M. Bordoni et al.

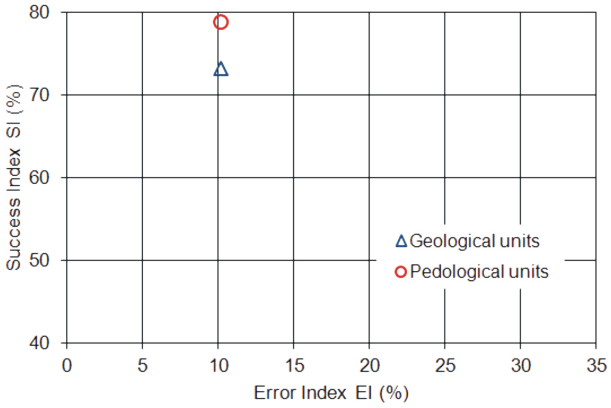

Figure 13. Success (SI) and Error (EI) Indexes obtained with the TRIGRS-Unsaturated model for different types of unit mapping.

NHESSD
2, 7409–7464, 2014

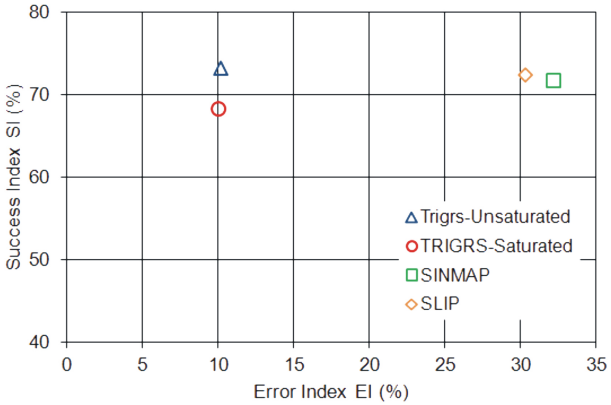

Figure 14. Success (SI) and Error (EI) Indexes obtained with the TRIGRS-Unsaturated, TRIGRS-Saturated, SINMAP and SLIP models for the study area considering a geological unit mapping.

NHESSD
2, 7409–7464, 2014